HEFAT2008
6th International Conference on Heat Transfer, Fluid Mechanics and Thermodynamics
30 June to 2 July 2008
Pretoria, South Africa
Paper number: HJ2

NUMERICAL SIMULATIONS OF FLUID FLOW THROUGH MODEL GEOMETRIES OF POROUS MEDIA
- at low to high Reynolds number -

Hellström J.G.I.* and Lundström T.S.
*Author for correspondence
Division of Fluid Mechanics,
Luleå University of Technology,
S-971 87 Luleå,
Sweden,
E-mail: gunnar.hellstrom@ltu.se

ABSTRACT

When modeling fluid flow through porous media it is necessary to know when to switch from a creeping flow formulation to a more elaborate laminar description or to a fully turbulent one. This is of importance in a large number of industrial processes such as flow through embankment dams, composites manufacturing, filtering and in the refinement of iron ore pellets. Regarding the creeping flow regime the Darcy law is sufficient while when inertia-effects become significant it is necessary to use the full Navier-Stokes equations or at least add a non-linear term to Darcy's law as done in the empirically derived Ergun equation, which has also turned out to be valid for some turbulent flows. It is however not obvious which equation to use at a certain Reynolds number and on what velocities and length scales Reynolds number should be based on. In order to shed some light on this Computational Fluid Dynamics is here applied to simple model geometries of porous media. In particular the flow through quadratic and hexagonal arrays of cylinders is studied. The main quantities of interest are the apparent permeability, the Blake-type friction factor as well as the forces acting on the cylinders. The simulations are carried out for a wide range of Reynolds number ranging from the creeping region to rather high Reynolds number flow, considering flow in porous media. The simulations are based on as well a laminar flow formulation as a turbulent one where the turbulence model chosen is the Shear Stress Transport model, and the CFD-software used is ANSYS CFX with extra care regarding grid resolution and numerical iteration in order to secure that the numerical errors are sufficiently small. One result is that inertia-effects become significant already at Reynolds number of about 10, for the quadratic packing, but around 50 for the hexagonal arrangement and the region where the laminar simulations differ considerably from the turbulent calculations is dependent on the different array arrangements.

INTRODUCTION

Ground water flows, flow through embankment dams, dewatering during paper-making, impregnation of fibre reinforcements during composites manufacturing and drying of iron ore pellets are a few examples where knowledge of flow through porous media is of highest importance. The flow characteristics will however vary as a function of pore geometry and ambient conditions. It is therefore of highest importance to derive general rules for when the flow field is transformed from one mode to another. In this context it is also of interest to elucidate the detailed flow field for different geometries. Both these issues will be here addressed. As long as the fluid is creeping in the pores Darcy's law applies according to

$$v_i = -\frac{K_{ij}}{\mu} p_{,j} \text{ and } \frac{Q}{A} = \frac{K}{\mu}\frac{\Delta p}{L} \qquad (1 \& 2)$$

where equation (1) represent the general form of Darcy's law and equation (2) the one-dimensional simplification. In these equations v_i is the superficial velocity, K_{ij} the permeability, μ the dynamic viscosity of the fluid, p the pressure, Q the volumetric flow rate through an area A and Δp the pressure drop over an length L in the stream-wise direction. The permeability is dependent on the geometry of the porous media as has, for instance, been described in the Kozeny-Carman equation

$$K = \frac{1}{B}\frac{\phi^3}{S^2(1-\phi)^2} \qquad (3)$$

where B is a constant, S the specific particle surface and ϕ is the porosity, [1]. For flow perpendicular to an array of cylinders Gebart [2] derived the following equation being valid as long as ϕ is small enough

$$K_{\perp} = C\left(\sqrt{\frac{1-\phi_{\min}}{1-\phi}}-1\right)^{5/2} R^2 \qquad (4)$$

where C and ϕ_{min} depends on the arrangement (such as quadratic or hexagonal).

However, when the flow in the pores becomes fully or partly turbulent an additional non-linear term is often introduced resulting in the so called Forchheimer equation

$$\frac{K}{\mu}\frac{\Delta p}{L} = \frac{Q}{A} + b\left(\frac{Q}{A}\right)^m \qquad (5)$$

where b is a property of the porous media and m is a measure of the influence of inertia [3]. Increasing the Reynolds number even more the flow becomes turbulent, or at least show turbulent-like behaviour, but experiments [1, 4] as well as numerical simulations [5] has indicated that it is possible to use equation (5) for this case as well. A modified and more engineering applicable version of equation (5) was presented by Ergun in 1952 by fittings to experimental data according to the following expression

$$\frac{\Delta p_f}{L} g = 150\frac{(1-\varepsilon)^2}{\varepsilon^3}\frac{\mu\dfrac{Q}{A}}{D_p^2} + 1.75\frac{1-\varepsilon}{\varepsilon^3}\frac{\rho\dfrac{Q}{A}}{D_p} \qquad (6)$$

where p_f is the pressure represented as a force, g is the gravitational constant, ε the fractional void volume in the bed, D_p the effective diameter of the particles and ρ the density of the fluid, [6]. The Ergun equation has shown best agreement with a bed of randomly distributed spheres and is therefore not optimal for all geometries, such as well structured arrays of material. The equation has therefore recently been generalised by Nemec and Levec to yield the following expression

$$\frac{\Delta p}{L}\frac{1}{\rho g} = \Psi = A\frac{\mathrm{Re}^*}{Ga^*} + B\frac{\mathrm{Re}^{*2}}{Ga^*} \qquad (7)$$

where A and B are tabulated material dependent constants. Experiments yield that the values of A and B range from 180 to 280 and 1.9 to 4.6 respectively. This rather huge variation indicates that the knowledge of the material in itself must be improved, [7], a topic that will be addressed in this study. The modified Reynolds and Galileo numbers appearing in equation (7) are defined as

$$\mathrm{Re}^* = \frac{\rho\varphi D_p U}{\mu(1-\varepsilon)} \text{ and } Ga^* = \frac{\rho^2 g\varphi^3 D_p^3\varepsilon^3}{\mu^2(1-\varepsilon)^3} \qquad (8 \& 9)$$

according to [8], where Re^* represents the true averaged velocity in the pores taking the pore volume fraction ε into account and including the tortuosity φ. The Galileo number in its turn gives us the ratio between the gravitational and viscous forces and is strongly dependent on particle diameter and pore volume fraction.

Another common way of relating pressure to flow rate is by the Blake-type friction factor that may be defined as:

$$f' = \frac{\Delta p}{L}\frac{D_p}{\rho\left(\dfrac{Q}{A}\right)^2}\frac{\phi^3}{1-\phi}. \qquad (10)$$

Introducing this relationship into the Ergun equation (6) results into the following expression

$$f' = 1.75 + \frac{150}{\mathrm{Re}'} \qquad (11)$$

which resembles experimental data and where the modified Reynolds number is defined as

$$\mathrm{Re}' = \frac{\rho D_p\dfrac{Q}{A}}{\mu}\frac{1}{1-\phi}. \qquad (12)$$

This way of expressing Re originates from the investigation performed by Ergun where Re is related to a diameter characteristic for the material [9]. There exist several formulations regarding Re where the description of the characteristic length, for instance, the diameter of a representative object in the media or the hydraulic diameter is used and also the velocity description differs.

Several researchers have investigated the validity of the equations described above where, for instance, the review-article by Hlushkou and Tallarek analyses the flow regions, creeping, viscous-inertial and turbulent, from a macro-scale transport behaviour point of view with the results that the laminar region end at a superficial Re at the order of 100, [4]. From an experimental study on a pore scale Lesage, Midoux and Latifi concluded that the flow is laminar for particle Re below 110 and turbulent for particle Re above 280, [10]. The influence of apparent permeability with respect to Re in periodic arrays is calculated by Edwards, Shapiro, Bar-Yoseph and Shapira indicating that the orientation-dependent permeabilities of both square and hexagonal monodisperse arrays are observed to diminish with the increase of Re, [11]. In the numerical investigation by Koch and Ladd the procedure to calculate the drag is elucidated for different arrays of cylinders.

It is, for instance, found that in random arrays, the drag makes a transition from quadratic to a linear Re-dependence at Re, based on the diameter of the cylinders and the average interstitial velocity, between 2 and 5, [12].

In this paper we perform similar numerical simulations with the aid of Computational Fluid Dynamics (CFD), in order to compare the flow through a well ordered porous material, an array of cylinders in quadratic and hexagonal packing, where the flow ranges from creeping region to fully turbulent. The simulations are performed both with a laminar and a turbulent description, the laminar approach was used in the laminar, viscous-inertial and the turbulent regions, and the turbulent approach in all three regions.

GOVERNING EQUATIONS

For the laminar set-up the following equations are used:

$$u_{i,t} + u_j u_{i,j} = -\frac{1}{\rho} p_{,i} + \nu u_{i,jj} \text{ and } u_{i,i} = 0 \quad (13 \& 14)$$

and for the turbulent part of the simulations the Navier-Stokes equations are Reynolds averaged resulting in the following equations:

$$U_{i,t} + U_j U_{i,j} = -\frac{1}{\rho} p_{,i} + \nu U_{i,jj} - \left(\overline{u_j u_i}\right)_{,j} \text{ and}$$

$$U_{i,i} = 0 \quad (15 \& 16)$$

where ν is the kinematic viscosity and $\overline{u_i u_j}$ are the Reynolds stresses. These equations represent the mean flow characteristics where turbulent effects are modelled via the Reynolds stresses, in order to obtain closure. The turbulence model chosen in this case is the Shear-Stress-Transport-model which is a combination of the k-ε and the k-ω models implying that the k-ω formulation is used in the near-wall region while the k-ε formulation is applied in the bulk where the shift takes place in the logarithmic part of the boundary layer. The mathematical formulation develops into the following non-trivial equations:

$$\frac{D\rho k}{Dt} = S_{ij}\frac{\partial u_i}{\partial x_j} - \beta^* \rho\omega k + \frac{\partial}{\partial x_j}\left(\left(\mu + \sigma_k \mu_T\right)\frac{\partial k}{\partial x_j}\right) \&$$

$$\frac{D\rho\omega}{Dt} = \frac{\gamma}{\nu_T} S_{ij}\frac{\partial u_i}{\partial x_j} - \beta\omega^2 + \frac{\partial}{\partial x_j}\left(\left(\mu + \sigma_\omega \mu_T\right)\frac{\partial \omega}{\partial x_j}\right) + 2\rho\left(1 - F_1\right)\sigma_{\omega 2}\frac{1}{\omega}\frac{\partial k}{\partial x_j}\frac{\partial \omega}{\partial x_j}$$

(17 & 18)

where k is the turbulent kinetic energy, S_{ij} the turbulent stress tensor, ω the turbulent frequency, μ_T the turbulent dynamic viscosity, ν_T the turbulent kinematic viscosity and β^*, σ_k, γ, σ_ω, F_1 and $\sigma_{\omega 2}$ are constants. A detailed description of the SST-model can be found in a number of papers and books on turbulent flows see, for instance, [13].

GEOMETRY AND NUMERICAL VERIFICATION

The geometries chosen for this investigation is infinitely long cylinders, packed in quadratic and hexagonal patterns, for which unit-cells are defined and divided into finite volumes with ANSYS ICEM CFD Hexa, see Figure 1.

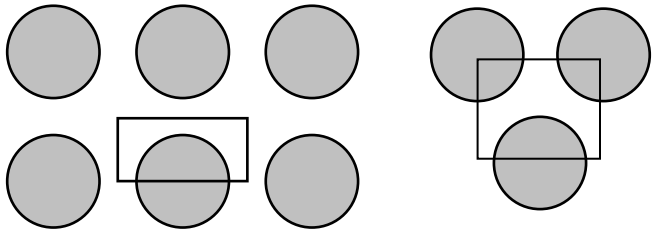

Figure 1 Schematic sketch of the computational domain

The software used for the simulations is ANSYS CFX and the grid chosen gives an error estimated to be less than 0.3 ‰ when using 370 000 nodes, [14]. Regarding the turbulent simulations measures are taken to keep the maximum y-plus low enough. To exemplify, for the simulation with Re' = 2 000 the maximum y-plus is 1.3 being in line with the recommendation in the CFX-manual saying that the y-plus should be lower than 2, [15], as well as the ERCOFTAC Best practice Guidelines 2000 stating that the y-plus should be below 4 and close to unity, [16]. The simulations are performed on a LINUX-cluster with HP-MPI-2.1 as the communication protocol and the partitioning applied is MeTis. Regarding the boundary conditions of the unit-cells the top and the bottom part are symmetry-planes, the cylinder walls are assumed to be smooth with a no-slip condition and the left and right hand sides are periodic domain interfaces all in all representing the repeatable structure of the array. To drive the flow in the unit-cell a momentum source is defined in a subdomain. The advection scheme used to solve the continuity and momentum equations are chosen to be strictly second order accurate by setting the specified blend factor equal to one in CFX-Pre. The simulations are furthermore assumed to be well converged when the Root Mean Square (RMS) residuals have dropped 5-6 orders of magnitude and when the maximum residuals are less than 1.5 orders of magnitude above the RMS-residuals. For the unsteady calculations a second order backward Euler scheme is applied and the time step is selected so that the Courant number is between 0 and 5. To discern the unsteady behaviour of the simulations a number of monitor-points were introduced recording pressure at nine locations and also logging the massflow at the domain interfaces. Regarding the turbulent initial conditions the turbulent kinetic energy was chosen to 0.03 m^2/s^2 and the eddy frequency is set to 300 Hz following experience from former simulations and post-processing. For the periodic domain interface boundaries the turbulence options is set as a conservative interface flux. To ensure that the selected values of the turbulent parameters are relevant for the

problem studied a perturbation analysis was carried out with the conclusion that the variations introduced only weekly influence the results indicating that the solutions obtained are stable in this context. At higher Reynolds number the simulations were performed by an unsteady approach since the steady simulations indicated problems like oscillating residuals and unstable values of the massflow. This was avoided by solving the flow with an unsteady approach instead. For the turbulent set-up these indications did not occur hence the steady approach throughout all the turbulent simulations performed, based on the stability in the monitor points for the sought variables.

RESULTS AND DISCUSSION

For the quadratic arrangement inertia becomes significant at a Reynolds number of about 10 independent of the porosity of the array, see the plots for the laminar set-up in Figure 2. This result is in conformity with data presented in the literature [4, 5, and 14] implying that we can put additional trust into our simulations as a complement to the mesh refinement studies performed. The next significant result is that the laminar and turbulent approaches give similar results up to a certain point where the solution of the turbulent formulation starts to give lower permeability data. Hence the point is found were the contribution to the overall losses from the modelled turbulence grows to be important as compared to the pure viscous ones and those that can be traced to inertia effects. If the turbulence models utilised follow the reality, as presented in [5], the on-set of turbulence for these particular geometries can be found. In contrary to inertia this on-set is dependent on the detailed geometry giving a characteristic Re' that varies from 200 to 700 for the porosities considered. This diversity can however be avoided if the Reynolds number is reformulated with the result that the on-set to turbulence is captured but then the inception of inertia becomes dependent on the Re' [5].

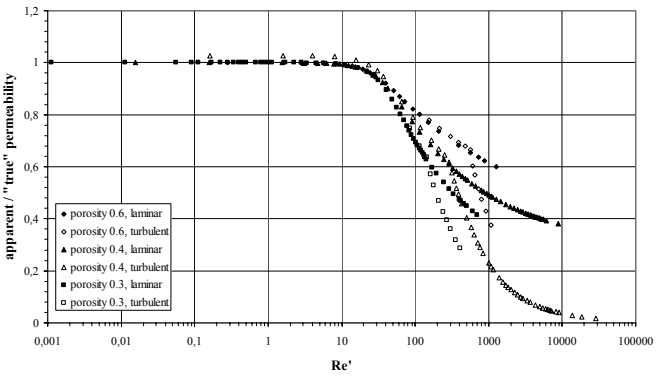

Figure 2 The apparent permeability divided by the true permeability for the quadratic arrangement with three porosities, 0.3, 0.4 and 0.6, with laminar setup as well as a turbulent one.

A third result of the simulations performed is that inertia comes into operation when Re' is about 50 for the hexagonal packing which considerably exceeds the value for the quadratic packing and those found in the literature, see Figure 3. Another feature of the simulations with the hexagonal array, being rather surprising, is that the laminar and turbulent formulations, in essence, give the same permeability values when Re' ranges from 0.02 to 8000, i.e. over the span tested. This indicates that turbulence is a second order effect for the losses in this range. A comparison of vector graphs for the two geometrical set-ups and for flow at high Reynolds numbers yields that the jet formed in the hexagonal array is not straight enabling a inertia dominating flow and the production of turbulent kinetic energy, k, is considerably lower strengthening the idea that turbulence is a second order effect for the hexagonal array of cylinders also for Reynolds numbers as high as 19 000, see Figures 4, 5, 6 and 7

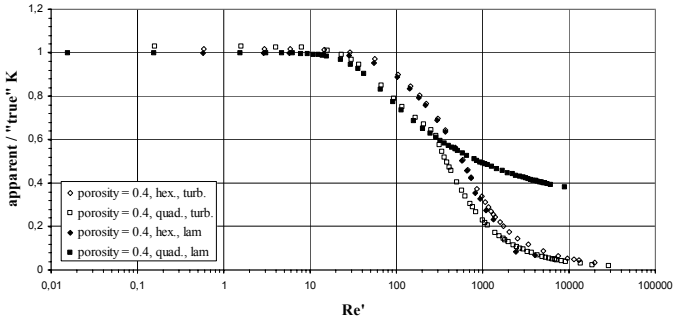

Figure 3 The apparent permeability divided by the true permeability quadratic and hexagonal packing at a porosity of 0.4, for the laminar and turbulent cases.

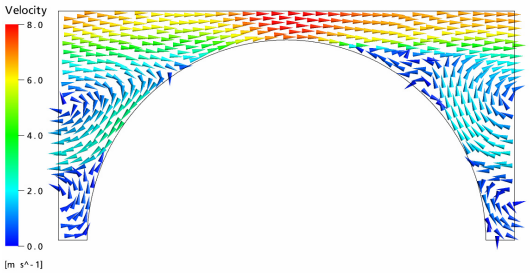

Figure 4 Vectors representing the velocity field for the turbulent configuration for the quadratic packing with porosity 0.4 and Re'=19 000.

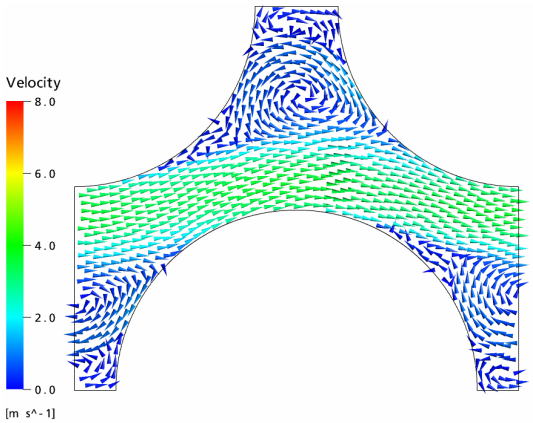

Figure 5 Vectors representing the velocity field for the turbulent configuration for the hexagonal packing with porosity 0.4 and Re'=19 000.

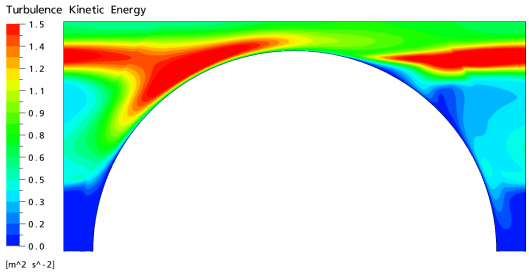

Figure 6 Contour plot of the turbulent kinetic energy for the turbulent configuration of the quadratic packing with porosity 0.4 and Re'=19 000.

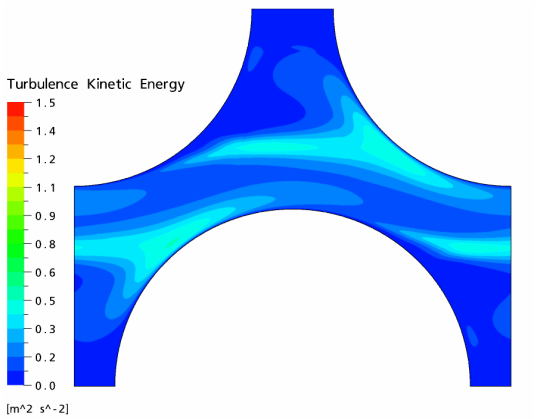

Figure 7 Contour plot of the turbulent kinetic energy for the turbulent configuration of the hexagonal packing with porosity 0.4 and Re'=19 000.

When comparing the numerical data with experiments from the literature, i.e. equations (6) and (7) by usage of the Blake-type friction factor, derived in equation (10) and (11) it is possible to see that the turbulent simulations of both the quadratic and hexagonal array level out just as the experimental results, although there is a shift in height, see Figure 8. The laminar simulations for the hexagonal geometry also levels out while those for the quadratic arrangement do not. These results show that the observed levelling out of the friction factor may be due to two mechanisms turbulence (quadratic packing) and extensive inertia (hexagonal packing).

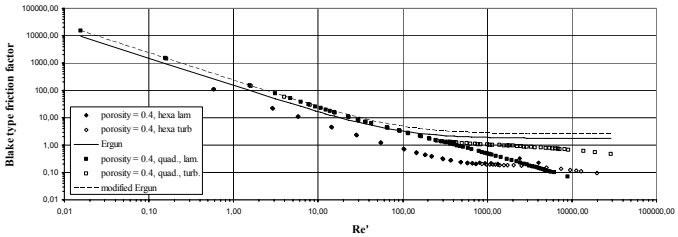

Figure 8 The Blake-type friction factor calculated for the simulations as well as the Ergun equation and the modification by Nemec and Levec for the quadratic and hexagonal packing.

When considering internal erosion processes in embankment dams, for instance, it is of importance to identify the forces acting on the material. By doing this on the cylinders it is clear that the dominant force is the normal forces and that the forces on the quadratic packed cylinders are higher as compared to the hexagonal packed ones, Figure 9 and 10. It can also be seen that for the quadratic packing the normal as well as the shear forces differ a lot when comparing the laminar with the turbulent results. The difference is much clearer than for the hexagonal setup.

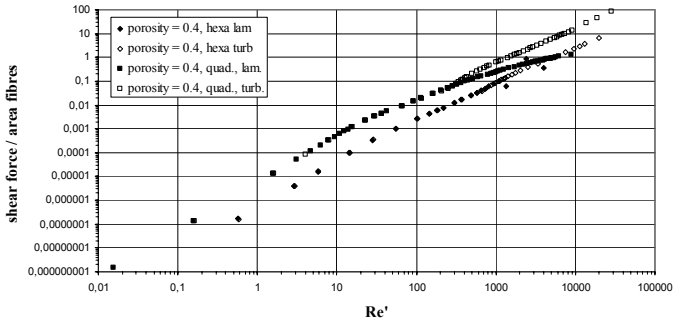

Figure 9 The shear force acting on the cylinder for both geometrical setups.

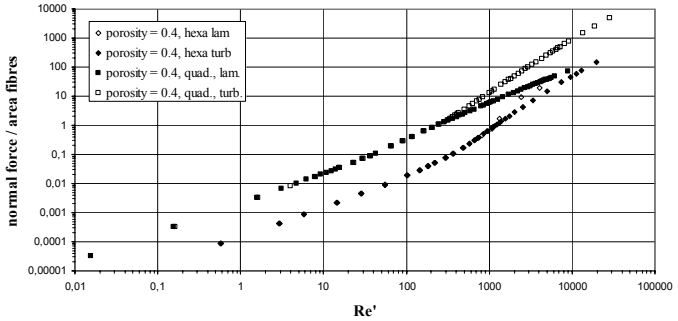

Figure 10 The normal force acting on the cylinders for both geometrical setups.

CONCLUSIONS

The difference between the quadratic and hexagonal geometrical arrangements is quite large when considering the prediction of permeability and the identification of the three flow regimes: Darcy flow, laminar inertia flow and turbulent flow. The identification of these regimes is apparent for the quadratic packing but for the hexagonal array, the turbulent flow regime, or the regime where turbulence is significant for the apparent permeability, is not found with the method used in this paper even if Re' is as large as 19 000. This can possible be traced to creation of inertia rather than turbulent kinetic energy as the fluid moves between the cylinders. It is also found that the Darcy flow regime stretches all the way to Re' = 50 for the hexagonal arrangement as compared to Re' = 10 for the quadratic ones. This is most likely due to the additional losses, for the quadratic case, which correspond to the velocity distribution difference. For the quadratic packing the Shear Stress Transport model seems to mimic the flow field in a satisfactory way all the way from low Reynolds number Darcy flow to turbulent ones although it is designed for high Reynolds

number flows. The Blake-type friction factor gives the same indication that for the hexagonal array, the laminar and turbulent setups level out for high Reynolds number, which is not observed for the quadratic array where the friction factor for the laminar setup is strictly linear throughout all the simulations. Finally the normal force on a cylinder is the dominant one as compared to the shear force.

ACKNOWLEDGEMENT

The research presented was carried out as a part of "Swedish Hydropower Centre – SVC". SVC has been established by the Swedish Energy Agency, Elforsk and Svenska Kraftnät together with Luleå University of Technology, The Royal Institute of Technology, Chalmers University of Technology and Uppsala University. www.svc.nu.

REFERENCES

[1] Bear, J., Dynamics of Fluids in Porous Media, *Dover publications Inc. New York,* 1972.

[2] Gebart, B. R., Permeability of unidirectional reinforcements for RTM, *Journal of Composite Materials*, Vol. 26, 1992, pp. 1100-1133.

[3] Forchheimer, P., Wasserbevegung durch Boden, *Z Ver. Deutsch Ing. 45*, 1901, pp 1782-1788.

[4] Hlushkou, D., and Tallarek, U., Transition from creeping via viscous-inertial to turbulent flow in fixed beds, *Journal of Chromatography*, Vol. 1126, 2006, pp. 70-85.

[5] Hellström, J. G. I., Jonsson, P. J. P., and Lundström, T. S., Numerical Study of Turbulent Flow through Porous Media, to be submitted.

[6] Ergun, S., Fluid flow through packed columns, *Chemical Engineering Progress*, Vol. 48, 1952, pp 89-94.

[7] Nemec, D., and Levec, J., Flow through packed bed reactors: 1. Single-phase flow, *Chemical Engineering Science*, Vol. 60, 2005, pp. 6947-6957.

[8] Niven, R. K., Physical insight into the Ergun and Wen & Yu equations for fluid flow in packed and fluidized beds, *Chemical Engineering Science,* Vol. 57, 2002, pp. 527-534.

[9] Ghaddar, C. K., On the permeability of unidirectional fibrous media: A parallel computational approach, *Phys. Fluids,* Vol. 7, 1995, No. 11, pp. 2563-2586.

[10] Lesage, F., Midoux, N. and Latifi, M. A., New local measurements of hydrodynamics in porous media, *Experiments in Fluids,* Vol. 37, 2004, pp. 257-262.

[11] Edwards, D. A., Shapiro, M., Bar-Yoseph, P. and Shapira, M., The influence of Reynolds number upon the apparent permeability of spatially periodic arrays of cylinders, *Phys. Fluids A,* Vol. 2, 1990, No. 1, pp. 45-55.

[12] Koch, D. L. and Ladd, A. J. C., Moderate Reynolds number flows through periodic and random arrays of aligned cylinders, *J. Fluid Mech.,* Vol. 349, 1997, pp. 31-66.

[13] Menter, F. R., Zonal two equation k-ω turbulence models for aerodynamic flows, *AIAA,* paper 93-2906, July 1993.

[14] Hellström, J. G. I. and Lundström, T. S., Flow through Porous Media at Moderate Reynolds Number, *Proceedings of the 4th International Scientific Colloquium Modelling for Material Processing,* Riga 2006, pp. 129-134.

[15] CFX® (Copyright© 1996-2005), Version 10.0, ANSYS Europe Ltd.

[16] ERCOFTAC (European Research Community On Flow, Turbulence And Combustion), Special Interest Group on Quality and Trust in Industrial CFD: Best Practice Guidelines, Version 1.0, 2000, edited by Casey, M. and Wintergerste, T.